agronomy

MDPI

Article

Spectral Variability Analysis of *Lupinus mutabilis* Sweet Under Nanofertilizer and Chelate Application Through Spectroscopy and Unmanned Aerial Vehicle (UAV) Multispectral Images

Izar Sinde-González [1,*], Erika Murgueitio-Herrera [2,3], César E. Falconí [4], Mariluz Gil-Docampo [5] and Theofilos Toulkeridis [6,7]

1 Departamento de Ingeniería Topográfica y Cartográfica, E.T.S.I. en Topografía, Geodesia y Cartografía, Universidad Politécnica de Madrid, C/Mercator 2, 28031 Madrid, Spain
2 Departamento de Ciencias de la Tierra, Universidad de las Fuerzas Armadas ESPE, Sangolquí 171103, Ecuador; esmurgueitio@espe.edu.ec
3 Centro de Nanociencia y Nanotecnología, Universidad de las Fuerzas Armadas ESPE, Sangolquí 171103, Ecuador
4 Departamento de Ciencias de la Vida, Carrera de Ingeniería Agropecuaria, Grupo de Investigación Diversidad y Restauración Agroecológica (DYRA), Universidad de las Fuerzas Armadas ESPE, IASA I, Sangolquí 171103, Ecuador; cefalconi@espe.edu.ec
5 Departamento de Ingeniería Agroforestal, Universidad de Santiago de Compostela, 27002 Lugo, Spain; ml.gil@usc.es
6 School of Geology, Aristotle University of Thessaloniki, 54124 Thessaloniki, Greece; ttoulke@geo.auth.gr
7 Universidad UDET, Quito 170301, Ecuador
* Correspondence: i.sinde@upm.es

Abstract: Lupin is an Andean legume that has gained importance in Ecuador due to the protein content in its grain. Nonetheless, in recent times the production of lupin has been affected by inadequate nutritional management. In order to avoid such circumstances, the current study spectrally analyzed lupin cultivation under the application of nanofertilizers and Fe and Zn chelates, within two controlled trials, using a radiometer spectrum, an active crop sensor and a multispectral sensor mounted on a UAV. Vegetation indices were generated and subsequently statistically analyzed using ANOVA and Tukey tests. In the field trial, the treatments lacked an indication of significant improvements, while in the greenhouse trial, the nanofertilizer treatments indicated better results compared to the control treatments. However, it was also determined that the application of nanofertilizers at a concentration of 540 ppm demonstrated significant efficiency in greenhouse conditions, which could not be achieved in the field. Furthermore, the chelate treatment presented a certain degree of toxicity for the plant.

Keywords: lupin; nanofertilizer; UAV; vegetation index; crop monitoring; spectral analysis; spectroscopy

Academic Editor: Andreas Stylianou, George Adamides, Damianos Neocleous and Christopher Brewster

Received: 14 January 2025
Revised: 7 February 2025
Accepted: 8 February 2025
Published: 14 February 2025

Citation: Sinde-González, I.; Murgueitio-Herrera, E.; Falconí, C.E.; Gil-Docampo, M.; Toulkeridis, T. Spectral Variability Analysis of *Lupinus mutabilis* Sweet Under Nanofertilizer and Chelate Application Through Spectroscopy and Unmanned Aerial Vehicle (UAV) Multispectral Images. *Agronomy* **2025**, *15*, 469. https://doi.org/10.3390/agronomy15020469

1. Introduction

Precision agriculture is understood as a set of techniques aimed at optimizing agricultural inputs according to the spatial and temporal variability of production, which is achieved with an adequate allocation of inputs depending on the needs and potential of each management area [1–4]. Therefore, in order to study, evaluate and understand spatial and temporal variations, it is indispensable to use technologies such as the global positioning system (GPS), satellites, remote sensors and images of the area, linked to geographic information systems (GISs) [5–10]. In this sense, precision agriculture provides georeferenced information through maps of soil fertility or yield. Using remote sensors, it

is then able to generate immediate information and optimally distribute agricultural inputs, satisfying food needs [11–14].

Nanotechnology focuses on the development, characterization and use of materials with very small dimensions, i.e., <100 nm [15–22]. In this group of materials are nanoparticles, which have great potential in agriculture as they are able to be used as nanofertilizers [23–31]. Nanofertilizers focus on the synthesis of macro and micro nutritive elements for crops, but mainly on micronutrients (Zn, Cu, Mn and Fe) [32–37]. Plants need mineral nutrients to complete their life cycle, since they are involved in metabolic functions and are part of their organic structures. These nutrients are classified according to their concentration; macronutrients are required in large quantities (N, P, K), and micronutrients are required in small amounts (Ca, Mg, S, Fe, Mn, B, Zn, Co, Mo), though they have the same importance as macronutrients [38–41]. Iron plays an essential role as a component of enzymes involved in the transfer of electrons in the process of photosynthesis [42,43]. The lack of this micronutrient can be observed in young leaves in the form of interveinal chlorosis, which reduces the synthesis of protein–chlorophyll complexes in chloroplasts, while the lack of zinc causes a reduction in the growth of internodes [44,45]. Subsequently, leaves may be small, deformed and present chlorosis (the latter between the nerves of older leaves) [46–50].

Lupin or chocho (*Lupinus mutabilis* Sweet) is an Andean legume with a high protein content (approximately 46% in dry grain) compared to other legumes and Andean cereals [51–56]. This legume provides phosphorus, iron and zinc, which are the main minerals in the human body; therefore, it is considered to be a product that contributes to the food sovereignty of many countries [57–61]. The lupin is part of a variety of agricultural products that have a fundamental nutritional content, as it has a high percentage of protein and other nutrients that are essential for human health and for food sovereignty in Ecuador [62–64]. In Ecuador, lupin cultivation is located in the highland region, where it is capable of adapting to different types of soil, especially in dry and sandy agro-ecological zones between 2600 and 3400 m above sea level (m a.s.l.) [65–67]. It develops in environments where rainfall fluctuates between 300 and 600 mm per year and with temperatures between 7 and 14 °C [68,69].

Anthracnose is a disease that affects stems, leaves, pods and seeds in all stages of lupin plant development. Therefore, this problem alters the spectral response of lupin and therefore its value in the NDVI vegetation index, which in turn allows researchers to evaluate the health of the given vegetation [70–74].

Remote sensing is a useful technology for precision agriculture—satellite platforms are very significant in the monitoring of agricultural production [75–78]. However, within agricultural-scale applications, they have not been adopted as expected, due to a variety of challenges such as pixel resolution, infrequent coverage, presence of clouds and frequently slow delivery of information to the corresponding users [79]. Nonetheless, unmanned aerial vehicles (UAVs) or drones provide a remote sensing platform with the ideal characteristics for data acquisition, such as high spatial resolution, on-demand coverage and fast information delivery [80–86].

Remote sensing, being a discipline that obtains information from an element by detecting and analyzing its radiated energy, lays its foundations in the study of spectroscopy [87]. This refers to the observation and study of the electromagnetic spectrum and is based on the interaction of radiant energy with matter, meaning that it measures the intensity of radiation as a function of the wavelength of an object [88]. That implies the determination of energy of many parts of the electromagnetic spectrum against matter, including vegetation. This allows researchers to monitor vegetation in a spatial and temporal way, allowing predictions of crop production, agricultural land use examination, as well as the early detection and control of crop diseases [89–94].

There have been several remote sensing studies focused on analyzing the spectral responses of various phenological stages of crops, such as those by [95] on grasslands and [96] on Mediterranean plants. There has also been a notable variety of research in the cultivation of lupin, where the spectral behavior of the crop was analyzed after seed disinfection and greenhouse and field implementation [97–99].

Based on the aforementioned context, the present study aims to determine the spectral variability in the phenological states of lupin crops in two controlled trials (greenhouse and field). The spectral analysis will focus on the effects of the addition of chelates and nanofertilizers for crop control and monitoring purposes.

2. Materials and Methods

2.1. Study Area

The study area is located in the central part of the Inter-Andean Valley, inside the highlands of continental Ecuador, a country characterized by complex geodynamic settings associated with a variety of natural hazards [100–102]. Two tests were conducted within Campus IASA I in the Prado farm of the University of the Armed Forces ESPE (Figure 1). The first test took place in a greenhouse with a translucent plastic cover and the second test in the field, with areas of 60 m^2 and 240 m^2, respectively. This zone has a humid mesothermic equatorial climate, with an average annual temperature of 14 °C. The average annual rainfall is about 1500 mm, due to the location being at an altitude of 2748 m a.s.l. The predominant soil type is mollisol, which is characterized by having a high content of organic matter.

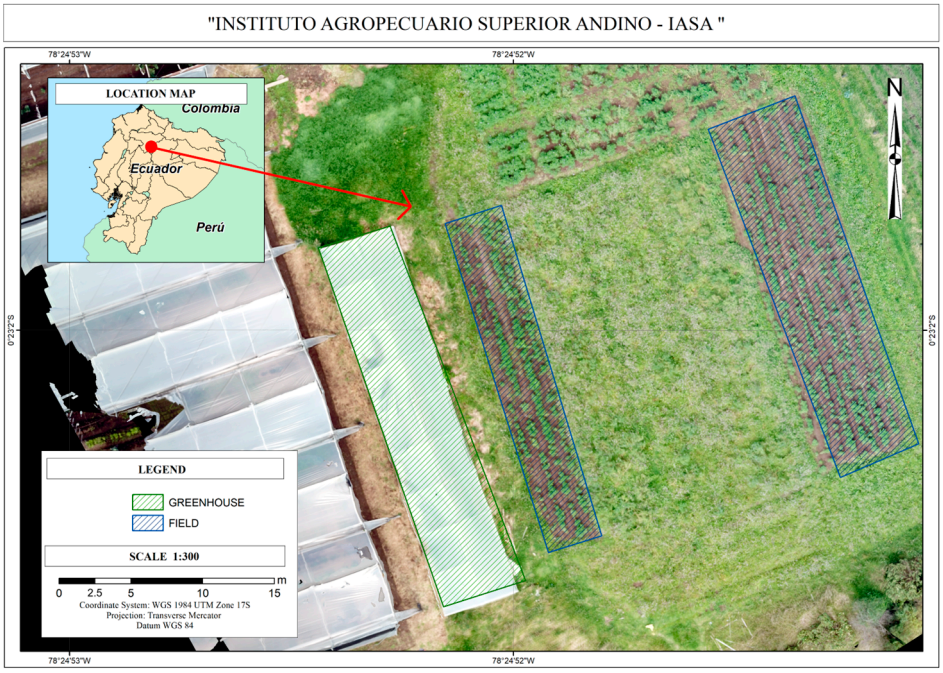

Figure 1. Location map of controlled trials.

2.2. Material

Spectral data were obtained with a Spectral Evolution PRS-1100 spectroradiometer, which records spectral information in a range of 320–1100 nm. In addition, a GreenSeeker crop sensor was used, which emits bursts of red and infrared light and measures the light reflected by the leaves of the crop, with which it was possible to obtain normalized difference vegetation index (NDVI) values. Furthermore, in order to obtain spectral information of the plant canopy, a DJI Mavic Pro UAV was used, where a multispectral sensor MAPIR

Survey 3W - Red + Green + NIR (RGN, NDVI) was mounted. With that sensor we were able to obtain information in near infrared (850 nm), red (660 nm) and green (550 nm) light. Control points were obtained using a precision Trimble R8 GPS. Qgis software (QGIS Development Team) was applied for geospatial data management. A diagram with the materials and general process is illustrated in Figure 2.

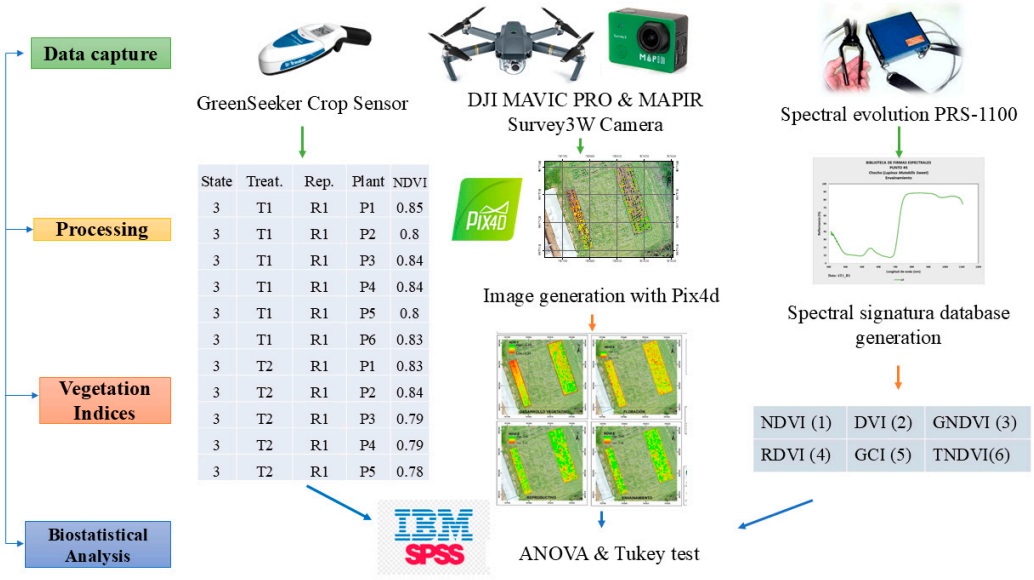

Figure 2. The schematized methodology flow diagram used in the present study.

The formulas for the Vegetation Indices calculation are:

$$NDVI = \frac{R_{nir} - R_{RED}}{R_{nir} + R_{RED}} \quad (1)$$

$$DVI = R_{nir} - R_{RED} \quad (2)$$

$$GNDVI = \frac{R_{nir} - R_{GREEN}}{R_{nir} - R_{GREEN}} \quad (3)$$

$$RDVI = \frac{R_{nir} - R_{RED}}{\sqrt{R_{nir} + R_{RED}}} \quad (4)$$

$$GCI = \frac{R_{nir}}{R_{GREEN}} - 1 \quad (5)$$

$$TNDVI = \sqrt{\frac{R_{nir} - R_{RED}}{R_{nir} + R_{RED}} + 0.5} \quad (6)$$

2.3. Establishment of Trials

Two trials were established in which the first was within a plastic greenhouse, with an approximate area of 60 m^2; the second was performed in the field, with an approximate area of 240 m^2. A completely random design (CRD) was applied with five treatments and three repetitions (R1, R2, R3), with a total of 15 experimental units per trial. In the greenhouse, each experimental unit had an approximate area of 4 m^2, while in the field each experimental unit included an area of approximately 15 m^2.

The project comprised five treatments, of which the first was the control (T1), the second and third treatment (T2 and T3) were the application of chelates of Fe and Zn at concentrations of 2 g/L and 4 g/L, respectively, while the fourth and fifth treatment (T4 and T5) were the application of nanofertilizers of Fe and Zn at concentrations of 540

ppm and 270 ppm, respectively. The treatments were applied using foliar spraying with the use of an atomizer, until the plant reached the point of runoff. In planning the sampling times, the phenology of the lupin was considered as a basis. Then, four samplings were conducted in the phenological stages of vegetative development, flowering, reproductive stage and sheathing. It should be noted that the samplings were performed between two and three days after the application of the treatments. The distribution of the trials in the greenhouse and field may be observed in Figure 3.

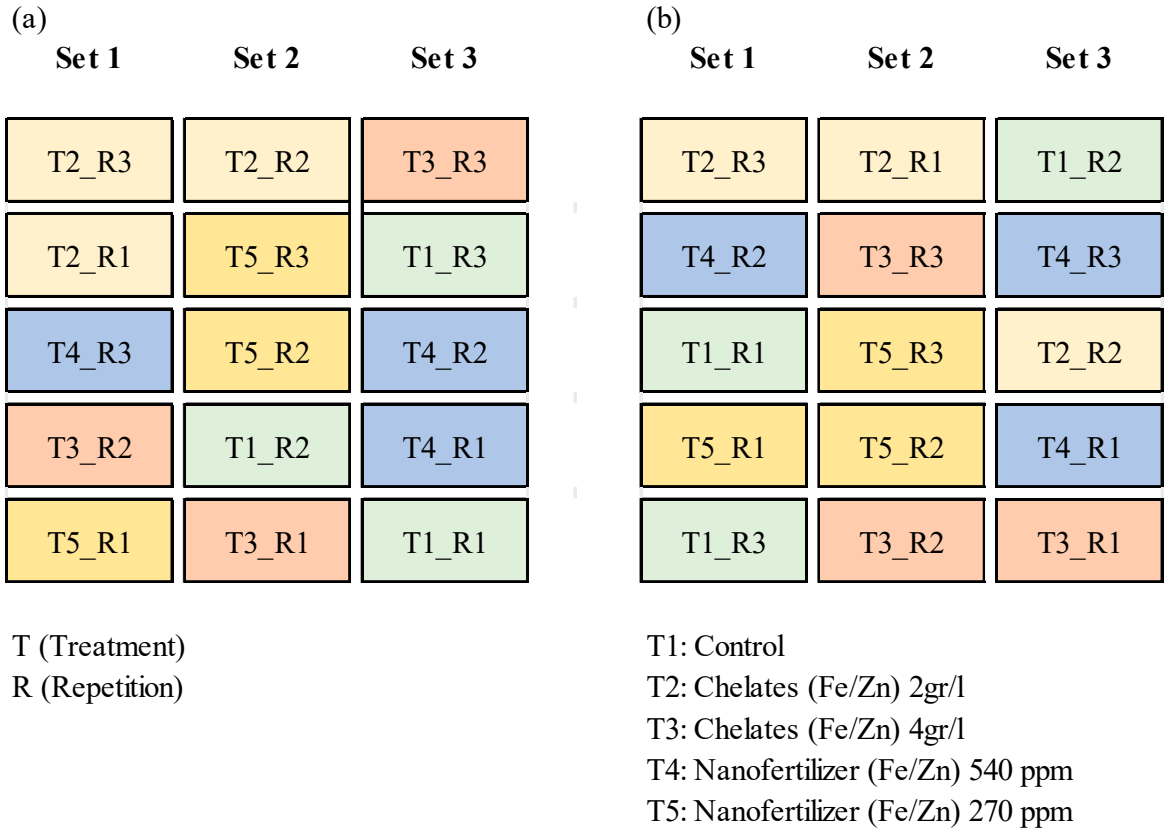

Figure 3. Distribution of treatments per experimental unit in (**a**) greenhouse and (**b**) field.

2.4. Data Capture

The data collection process was conducted between September 2019 and February 2020. The spectroradiometer was used to capture spectral data in the two trials. In each experimental unit, ten plants were selected, and from each one three leaves were chosen from the upper third of the plant. Therefore, thirty spectral data were obtained per experimental unit, and this process was repeated in the different samplings. The spectrum radiometer generates a file with a .sed extension, which is compatible with Microsoft Excel software. In Microsoft Excel, databases were set up according to the repetitions, treatments and phenological states of the three spectral values of each plant. The mean values of each were then derived, resulting in ten values for each experimental unit. The measurements were conducted in active mode, allowing the spectroradiometer to generate its own light source; thus, it was possible to eliminate environmental effects on the measurements.

Using the crop sensor, NDVI values were automatically obtained both in the field and in the greenhouse. In order to ensure the accuracy of the readings, the sensor was placed at a distance between 60–120 cm above the crop, parallel to the ground. In this way, in each experimental unit a value was taken per plant, resulting in 10 NDVI data for each unit in the different samplings. This equipment used has been illustrated in Figure 4.

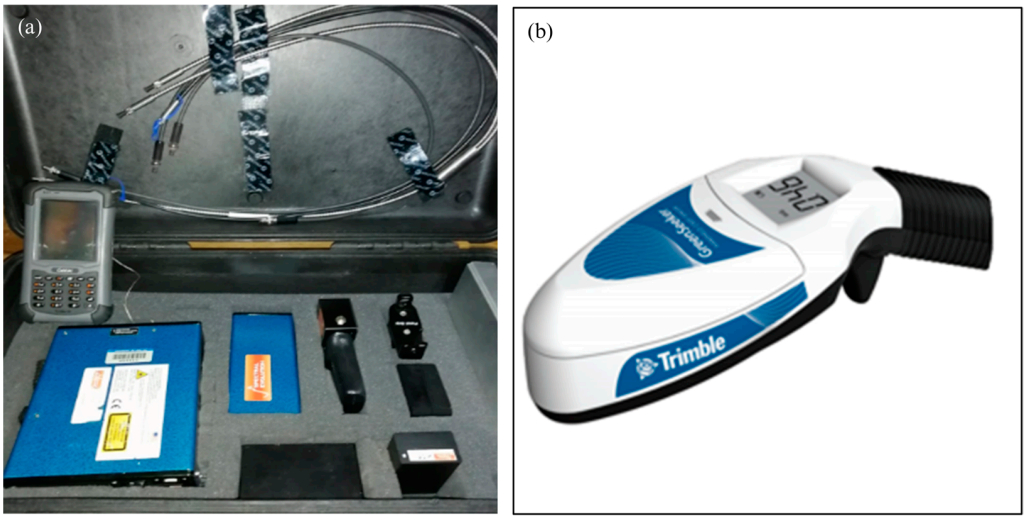

Figure 4. Equipment for data acquisition (**a**) PRS-1100 spectrum radiometer (**b**) GreenSeeker sensor.

2.5. Aerial Image Capture with UAV

With the use of the UAV, the aim was to explore the possibility of its future application as a tool for analyzing the effect of nanofertilizers on larger-scale crops. Therefore, in the field trial, a total of five flights were performed with the DJI Mavic Pro UAV and a Survey 3W - Red + Green + NIR camera, allowing us to take multispectral images on the same days as spectral data collection. For the execution of the flight, the Pix4D Capture application was realized, in which the flight parameters such as longitudinal and transverse overlap, height and terrain area were established. In order to georeference the multispectral images obtained, four control points were established, and subsequently materialized in cylindrical landmarks 40 cm high and 10 cm in diameter. The flights were tracked for two and a half hours each in static mode, and later post-processed using the ppp method.

In the processing of the images obtained, the Pix4Dmapper software was used with the 3D Maps template, which is capable of generating orthomosaics. The process is divided into three steps, being initial processing, mesh and point cloud generation and MDS and orthomosaic generation. Once the orthomosaics had been generated, the radiometric calibration was performed using the MAPIR Camera Control application and the MAPIR Calibration Ground Target PackageV2 card (See Figure 5). This process was repeated for the different flights in order to obtain orthomosaics in different phenological stages. A detailed explanation of the calibration process using the aforementioned software can be found in [103].

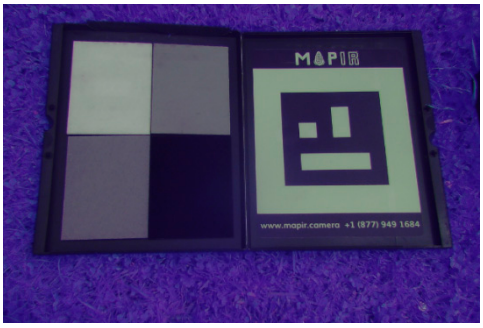

Figure 5. Calibration target V2 (MAPIR).

2.6. Generation of Vegetation Indices

The vegetation indexes, i.e., the normalized difference vegetation index (NDVI), transformed normalized difference vegetation index (TNDVI), green band (GNDVI), grassland curing index (GCI), renormalized difference vegetation index (RDVI), relative vigor

index (RVI) and difference vegetation index (DVI), were calculated from the spectral data [104–107]. This method involved extracting reflectance values from the entire spectrum captured by the spectroradiometer, specifically from the bands relevant to each vegetation index. With these values, the index can be calculated, which is a numerical value that enables the application of differentiation statistics and facilitates informed decision-making. Additionally, the DVI index was used to discriminate between soil and plant values, with the aim of avoiding values that could potentially contaminate subsequent extractions (See Figure 6). In the multispectral images obtained, the NDVI index was calculated. To obtain the value of the vegetation index per plant, they were georeferenced using the RTK method, with which 150 points were obtained (See Figure 7). A buffer was generated at these points and the Zonal Statistics tool was applied.

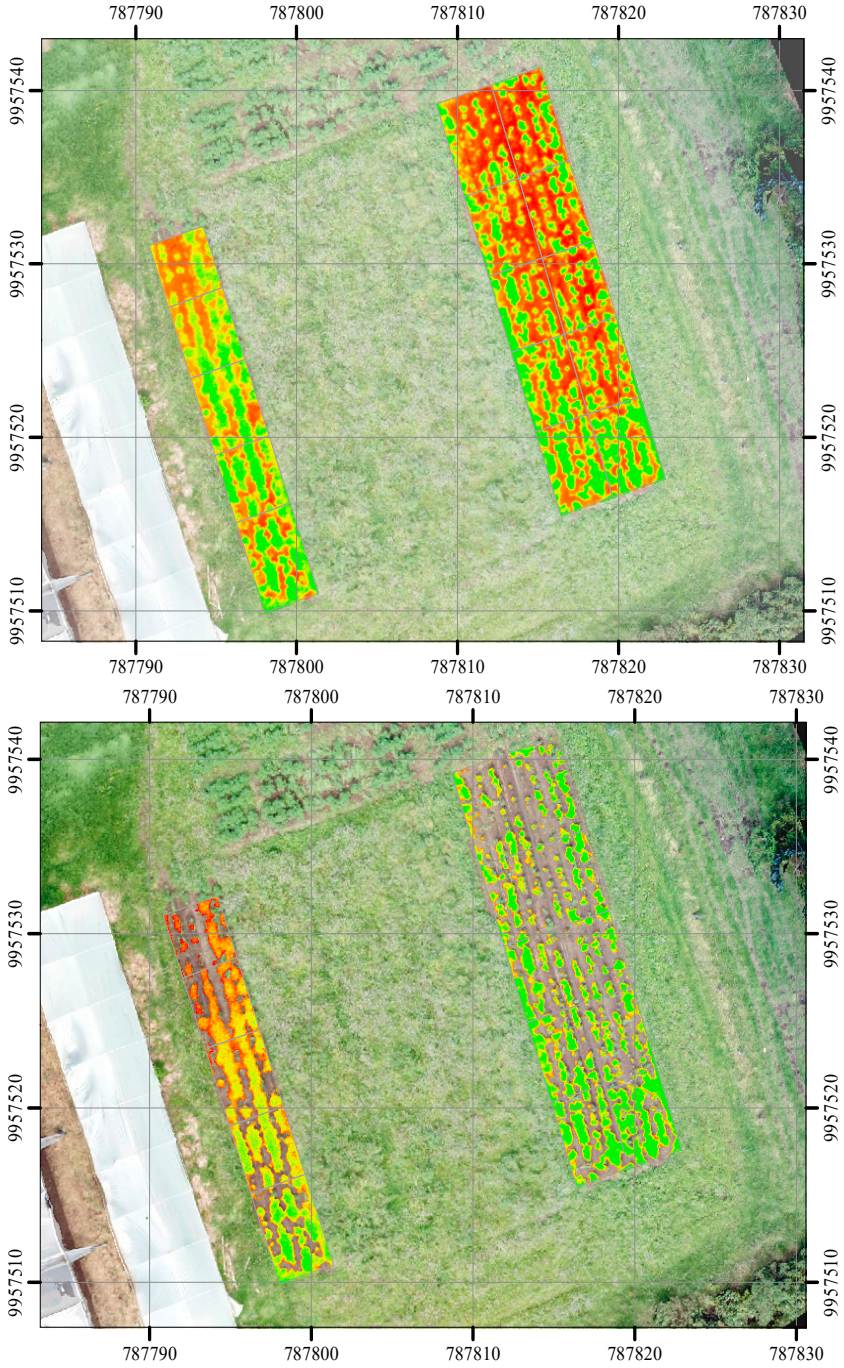

Figure 6. Discrimination between plant and soil pixels.

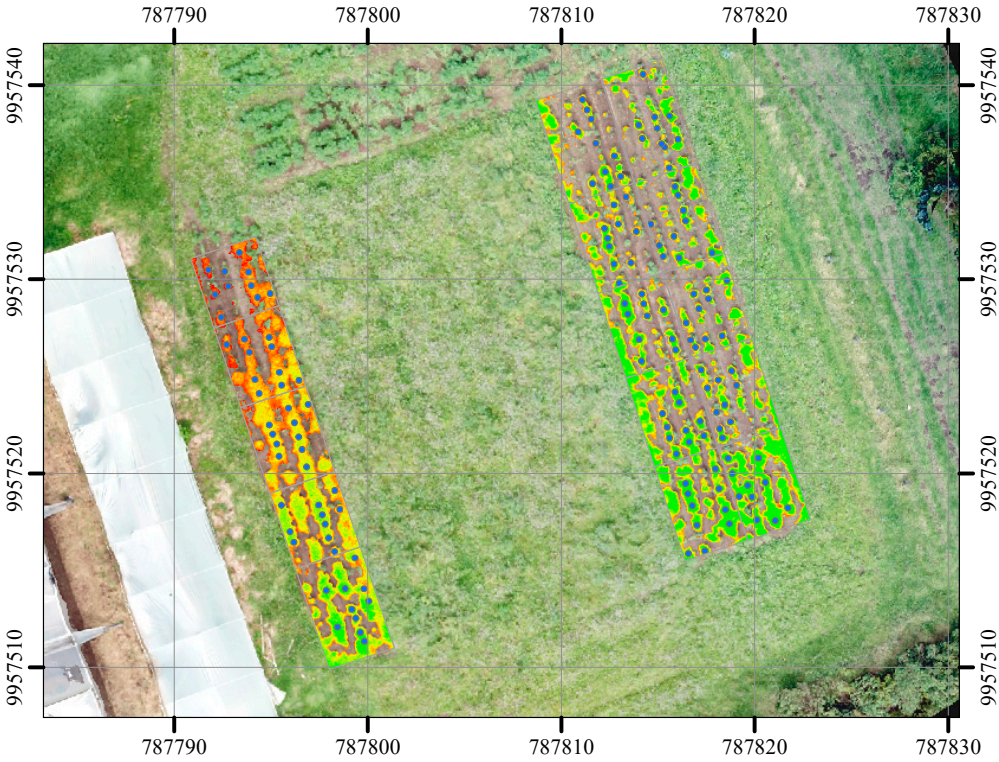

Figure 7. RTK plant positioning and NDVI index with mask.

2.7. Statistic Analysis

Prior to the ANOVA analysis of the vegetation index values obtained by different methods, an exploratory analysis of the data was conducted. This was generated in order to organize and prepare the data, detect failures in the data collection and identify outliers. Specifically, to ensure the validity of the statistical analyses, the assumptions of normality and homogeneity of variances were evaluated prior applying the parametric ANOVA test. Given that the dataset contained more than 50 observations, the Kolmogorov–Smirnov test was applied to assess normality, while Levene's test was employed to verify variance homogeneity. Additionally, outliers attributable to measurement errors were identified and subsequently excluded in order to prevent potential distortions within the results. The statistical analysis started with the hypothesis tests approach between the different treatments applied to the cultivation of lupin. Several hypotheses were then raised for both trials. Regarding the treatments, it is confirmed that H_0 are the vegetation indices that are not efficient to identify characteristics associated with the treatment of nanofertilizers and Fe and Zn chelates in lupin cultivation. The H_1 are the vegetation indices that are efficient to identify characteristics associated with the treatment of nanofertilizers and Fe and Zn chelates in the lupin crop. Regarding the phenological states, the H_0 are the vegetation indices which are not efficient to spectrally characterize the lupin crop during its phenological development. Finally, the H_1 are the vegetation indices which are efficient to spectrally characterize the lupin crop during its phenological development.

3. Results

3.1. Data Capture

A total of 1782 spectral signatures were obtained with the spectroradiometer in the trial, associated with the four samplings conducted, during the phenological development of the lupin. Regaring the NDVI index values, by using the crop sensor, a total of 600

values and 594 values were obtained for field and greenhouse trials, respectively. In the field trial, four orthomosaics were obtained in RGN, one for each phenological state during the development of the crop. The flight parameters were identical for all flights (Table 1).

Table 1. Flight parameters.

Flight time	6 min 59 s
Longitudinal overlap	90%
Transverse overlap	80%
Flight height	30 m
Total surface	37 m × 82 m
GSD	1 cm
Speed	3 m/s
Flight lines	5

3.2. Statistical Analysis of the Vegetation Index

Vegetation indices were calculated (NDVIE, GNDVI, TNDVI, DVI, RVU, RDVI and GCI) by means of the spectral response and NDVIS of the crop sensor, for each treatment, during the four phenological stages (reproductive stage, vegetative development, flowering and sheathing). From the images taken with the UAV in the field trial, a NDVIUAV map was produced for each phenological stage. From this information, descriptive statistics such as the mean, standard deviation, data distribution graphs and box plot were obtained. The analysis was performed in order to verify the existence of a normal distribution among the data and to obtain outliers.

3.3. Analysis of Variance (ANOVA)

For the field and greenhouse tests, an analysis of variance was applied to the vegetation indices obtained from the radiometric data, NDVIS values from the crop sensor and $NDVI_{UAV}$ values acquired through the UAV. This was in order to determine the hypotheses raised and to identify differences between the treatments and phenological states in the lupin crop, starting from the VI. Table 2 lists the treatment values and phenological states resulting from the trial.

Table 2. The *p*-values for vegetation indices (NDVIS)—greenhouse test.

Index		***p*-Value**	
		Treatment	**Phenological State**
Spectra	$NDVI_E$	<0.0001 *	<0.0001 *
	RVI	<0.0001 *	<0.0001 *
	GNVI	<0.0009 *	<0.0001 *
	TNDVI	<0.0001 *	<0.0001 *
	RDVI	<0.0001 *	<0.0001 *
	DVI	<0.0001 *	<0.0001 *
	GCI	<0.0032 *	<0.0001 *
Crop sensor	$NDVI_S$	0.5149	<0.0001 *

* Statistical significance *p*-value < 0.05.

Table 2 indicates that there is statistical significance in the vegetation indices when analyzing the treatments and phenological states of the lupin crop; therefore, the alternative

hypothesis is accepted. For the NDVI obtained with the crop sensor, there is no statistical difference in the treatment of chelates and nanofertilizers of Fe and Zn; therefore, the null hypothesis is accepted. However, for the case of phenological states, there is statistical significance; thus, the previously exposed alternative hypothesis is accepted.

The *p*-values presented in Table 3 indicate that the only statistically significant results were obtained from the RDVI, DVI and GCI indices through the application of nanofertilizers and chelates. Therefore, the alternative hypothesis was accepted. In the case of phenological states, the *p*-values indicate statistical significance in all indices, and therefore the previously exposed alternative hypothesis was accepted. For the NDVIUAV and NDVIS indices, statistical significance was found in treatments and phenological status. Once the indices were established with *p*-values < 0.05, Tukey's test was applied at 5% in order to find differences in means between the treatments and phenological states.

Table 3. The *p*-values for vegetation indices (NDVIUAV, NDVIS)—field trial.

		***p*-Value**	
	Index	**Treatment**	**Phenological State**
Spectra	$NDVI_E$	0.1835	<0.0001 *
	TNDVI	0.2001	<0.0001 *
	GNDVI	0.0831	<0.0001 *
	RVI	0.7576	<0.0001 *
	RDVI	<0.0001 *	<0.0001 *
	DVI	<0.0001 *	<0.0001 *
	GCI	<0.0141 *	<0.0001 *
UAV	$NDVI_{UAV}$	<0.0331 *	<0.0001 *
Crop sensor	$NDVI_S$	<0.0035 *	<0.0001 *

* Statistical significance *p*-value < 0.05.

3.4. Tukey's Statistical Test

3.4.1. Greenhouse Treatments

The NDVIE and TNDVI vegetation indices behave in a similar way; therefore, the results of the Tukey test indicate that treatments 2, 4 and 5 (T2, T4 and T5) occupy the same range (A). That is, statistically they are equivalent, while treatment 1 (control) occupies a different rank (B). This demonstrates that spectrally, it is possible to differentiate between a lupin plant with and without fertilizers (chelates and nanofertilizers). However, a difference cannot be established between nanofertilizer and chelate treatments, since they are statistically equivalent.

The results of the Tukey test of the GNDVI and GCI vegetation indices indicate that treatment T5 occupies one range (A), while treatments 2 and 3 (T2 and T3) occupy a different range (B), that is, they are statistically equivalent. However, treatments 1 and 4 (T1 and T4) can be located in A or B. Vegetation indices DVI and RDVI behave in a similar way. The results of the Tukey test demonstrate that treatment 4 (T4) occupies range (A), and treatments 1, 3 and 5 (T1, T3 and T5) occupy a different range (B); that is, statistically they are equivalent, while treatment 2 (T2) may be located in A or B.

3.4.2. Phenological States—Greenhouse

The results of the Tukey test of the NDVIE and TNDVI vegetation indices indicate that phenological stages 3 (vegetative development), 4 (flowering) and 6 (sheath-

ing) can be classified into three different categories (A, B and C), while phenological state 5 (reproductive) can be located in B or C, which allows us to deduce that the lupin crop can be differentiated spectrally by phenological state. The Tukey's test results of the GNDVI and GCI vegetation indices demonstrate that phenological stage 6 (sheathing) presents a range (B), while phenological stages 3, 4 and 5 occupy a different range (A). This indicates that spectrally it is possible to differentiate between the phenological states of the lupin crop. However, a difference cannot be established between states 3, 4 and 5, as they are statistically equal. In the case of the DVI and RDVI vegetation indices, it is evident that the four phenological states analyzed occupy a different range, which allows us to deduce that, spectrally, the lupin crop can be differentiated by phenological state, as listed in Table 4.

Table 4. Tukey test at 5% of the DVI and RDVI indices for the phenological stages in the greenhouse trial.

Phenological State	Description	DVI	RDVI	Range			
		Mean	Mean				
5	Reproductive	85.46	8.62	A			
3	Vegetative development	82.72	8.49		B		
4	Flowering	77.41	8.23			C	
6	Sheathing	76.02	8.11				D

Means with a common letter are not significantly different ($p > 0.05$).

3.4.3. Field Treatments

Regarding the application of the Tukey test on the RDVI values, the means of each treatment are demonstrated, e.g., treatment T1 belongs to range (A), followed by T5, while T4 is included in range (B). Therefore, there is no significant difference between their means, as the T2 treatment is in the (B–C) ranges, while the T3 treatment appears in the C range. The DVI index describes a grouping of treatments similar to the RDVI, because it was proposed to improve the DVI and NDVI indices. In this case, the T5 treatment is in the (A–B) ranges, meaning that there is no significant difference between the control and Fe and Zn nanofertilizers at 270 ppm concentration.

Tukey's test applied to the GCI index indicates that treatment T2 presented the highest mean, while treatment T5 and T1 are in the (A–B) ranges, coinciding with the DVI index. Hereby, there is no significant difference. On the other hand, there is a difference between treatment T2 and T4 with respect to T3. For the NDVI obtained from the crop sensor, it presents two ranges, the treatments T4 and T1 being in range (A), the treatments T5 and T2 in ranges (A–B), while range (B) includes the treatment T3. In other words, there is only a significant difference between the treatment T4, T1 with respect to T3, this being the lowest mean and it coincides with the rest of the indices in this aspect. The results of the Tukey test for the NDVIUAV index indicates that there is a significant difference only between treatments T3 and T1, with T3 being the maximum mean of all treatments, thus, this result differs from the rest of the indices analyzed.

3.4.4. Phenological States—Field

Tukey's test by phenological state, applied to the NDVIE and TNDVI indices, yields equal ranges for the means. Three ranges are identified, in which state 5 is in range (A), states 4 and 6 in range (B), and finally, state 3 in range (C). This confirms that the NDVIE and TNDVI indices identify spectral characteristics that differentiate between the phenological stages of the lupin crop. Tukey's test of the RDVI and DVI indices indicates a distribution of ranges similar to the NDVIE index, with three ranges where states 4 and 3 are significantly distinguished, while states 5 and 6 are in the same range. The behavior of the RDVI values

indicates that state 4 presents the highest mean compared to the NDVI index, which was state 5. Additionally, there is no significant difference between the last two states (5 and 6). The GNDVI and GCI indices (Table 5) presented a behavior similar to the previously described NDVIE index, and additionally coincides with the NDVIUAV, since state 5 is the highest mean. Thus, the hypothesis raised is corroborated, that the indices are efficient to spectrally characterize the lupin crop during its phenological development.

Table 5. Tukey's test for GNDVI, GCI indices by phenological state.

Phenological State	Description	GNDVI Mean	GCI Mean	Range			
5	Reproductive	0.73	5.44	A			
4	Flowering	0.70	4.64		B		
3	Vegetative development	0.68	4.20			C	
6	Sheathing	0.66	3.98				D

Means with one letter in common are not significantly different ($p < 0.05$).

The Tukey test for the NDVI values obtained from the GreenSeeker crop sensor demonstrates the means of the different phenological states, and they were classified into three ranges. There is a significant difference between states 3 and 6, while states 5 and 4 are not distinguished. Tukey's test for the NDVI values obtained by the UAV indicates four ranges, one for each phenological state (Table 6). That means that the stages of phenological development of the lupin crop are significantly distinguished, unlike what was shown by the NDVIE index, which did not present a significant difference between stages 4 and 6.

Table 6. Tukey's test for NDVIUAV index by phenological state.

Phenological State	Description	NDVI Mean	Range			
5	Reproductive	0.63	A			
3	Vegetative development	0.59		B		
6	Sheathing	0.53			C	
4	Flowering	0.35				D

Means with one letter in common are not significantly different ($p < 0.05$).

3.5. Comparison of NDVIS Values Between Trials

From the data obtained from the crop sensor, graphs illustrating the behavior of each treatment in the different phenological states for each trial are presented in order to perform a comparative analysis between trials (Figure 8). From the first application of nanofertilizers and chelates, an improvement was identified in the T4 and T5 treatments with respect to the initial state in the two trials. On the other hand, the T3 treatment indicates a decrease in the NDVI value for the field test, while it is maintained for the greenhouse test. The phenological state of flowering demonstrates a decrease in the NDVI value in all treatments, which is due to the susceptibility to diseases that this state presents. For both trials, treatment T4 shows a recovery compared to the rest. Finally, in the sheathed state, the treatments with nanofertilizers indicate higher averages than the control. Treatment T3 presented the lowest means throughout the vegetative development of the lupin crop.

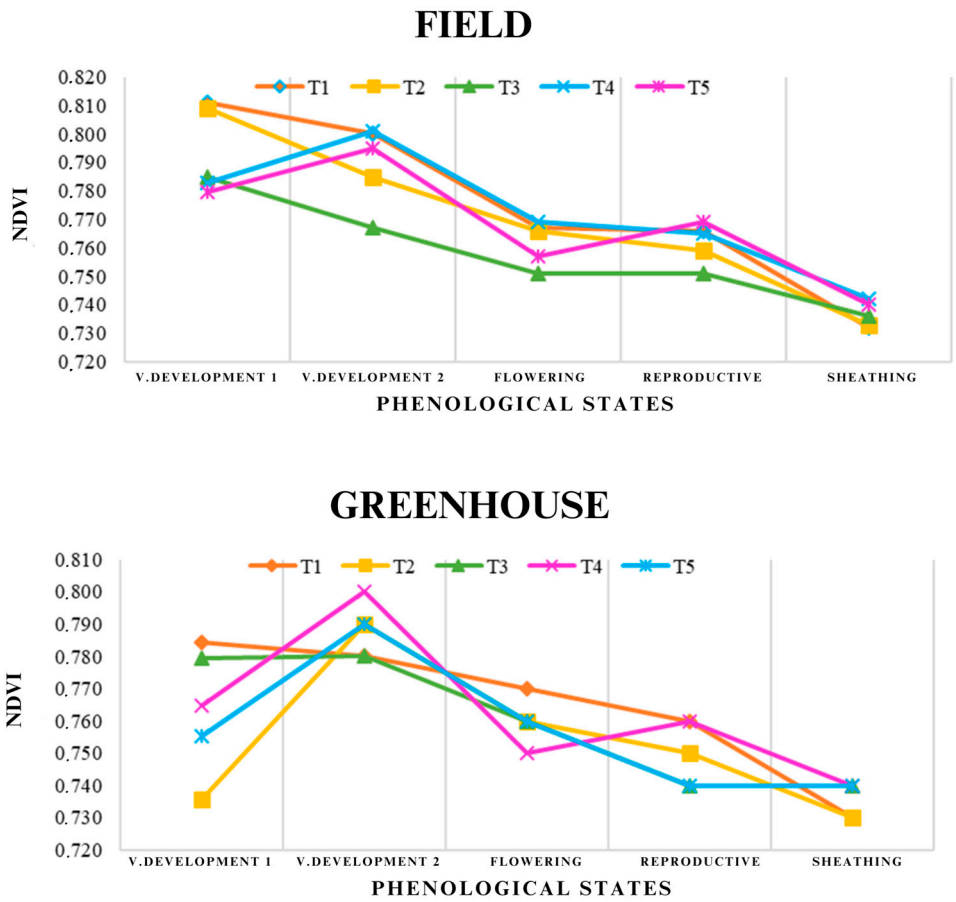

Figure 8. Treatment behavior for phenological stages in the field and greenhouse tests.

4. Discussion

4.1. Greenhouse Trials

Treatments

Data were generated from a spectroradiometer, a crop sensor and an UAV with a modified lens in order to generate vegetation indices (NDVI, TNDVI, SR-RE, NDRE, NDVIE and CCI). Within the studies previously mentioned, the NDVI and TNDVI indices did not efficiently identify significant differences between treatments, while in the current investigation these indices indicated that there is a significant difference between treatments T2, T3, T4 and T5, with respect to T1 (control).

In the case of the GNDVI and GCI indices, it was observed that treatment 2 (T2) presents the lowest value, while treatment 5 (T5) presents the highest. The GCI and GNDVI indices present a higher value in both treatment 5 and 4, because these indices have indicated greater sensitivity to variations in chlorophyll content. The RDVI and DVI vegetation indices demonstrate that treatment 1 has the lowest value, while T4 has the highest. These indices, by making use of the red and near-infrared portions of the electromagnetic spectrum, can establish reflectance combinations that are sensitive to chlorophyll concentration, foliage agglomeration and canopy leaf area. The effect of nanofertilizers on lupin cultivation may contribute to decreases in NIR wavelengths and increase in red wavelengths, thus causing an increase in the values of these vegetation indices [108].

In several studies conducted by applying the vegetation indices NDVI and TNDVI, significant differences were established between the phenological states of the crop, but with little precision; that is, one phenological state could not be differentiated from the other [99,109]. Similarly, in such studies the NDVI and TNDVI indices presented the same

results, but unlike previous studies, when applying the DVI and RDVI vegetation indices it was possible to establish significant differences in the four phenological stages of the crop.

4.2. Field Trial

4.2.1. Treatments

In the study of [109], significant differences were encountered between seed fertilization treatments applied to lupin cultivation through the NDVI and TNDVI indices obtained from spectral data. However, in the present project, these indices did not indicate any significant differences between the treatments applied for the field trial, and, on the other hand, the DVI, RDVI and GCI indices were able to significantly differentiate the applied treatments. According to the DVI and RDVI indices, both nanofertilizers and chelates were unable to present improvements with respect to the control. This differs from another study on the foliar application of the NPK nanofertilizer in potatoes, where significant effects on the yield and quality of the crop were reported [110]. The months in which the experiment was conducted corresponded to the wet season, accumulating 1370 mm of precipitation. Therefore, this lack of effect may be attributed to the possibility that rainfall washed away the foliar application.

According to the Tukey test for the GCI index, the T4 treatment indicates a higher mean than the control treatment. This was seen in a previous study, where ZnO nanofertilizers were sprayed on bean plants, generating important improvements in plant biomass, root length and chlorophyll content [111]. From the results obtained in the field, based on the Tukey test for the NDVIS and NDVIUAV indices, both indices significantly distinguished between applied treatments. Additionally, they presented a strong contrast, since in the NDVIS index, the treatment with the lowest mean was T3, the opposite of the NDVIUAV index, in the case of the crop sensor. This difference may be related to the data collection height, since the crop sensor performs readings of the upper part of the canopy of the studied plant. That is, the reflected energy detected belongs to the cover closest to the sensor, while the radiation or obtained from the images by UAV comes from the entire crop canopy [112].

In the field trial, the NDVI and TNDVI indices obtained from radiometric data significantly distinguished three of the four phenological states studied, indicating greater precision than in the study by [109], where only two phenological states with the same indices were differentiated. It also presents a precision similar to that indicated by [99] in their study on lupin using the NDVI and TNDVI indices obtained from radiometric data in a field trial. On the other hand, the RDVI and DVI indices significantly differentiated three states, as did the NDVI. The reproductive state presented the highest NDVI value, while the flowering state was the highest in DVI and RDVI. This contrast may be due to the fact that the NDVI index is more sensitive to low and medium concentrations of chlorophyll than RDVI, and the presence of chlorophyll in the leaves is closely related to plant health [113,114]. Finally, the GNDVI and GCI indices indicated greater precision compared to the rest of the indices obtained from radiometric data, since they significantly distinguished each phenological state. This coincides with the study by [99], where the authors analyzed the CCI index to distinguish between phenological states in lupin cultivation.

The NDVIUAV index significantly differentiated each phenological state, unlike the study by [99], where they demonstrated significant differences in only one phenological state. This may be related to the type of camera used (Parrot Sequoia); in the present study, a UAV camera was used. Regarding the behavior of the NDVIUAV value throughout the vegetative development, it was observed that the flowering state presented the lowest average, which was also seen by [115] in their study on corn. The value of the NDVI index presented greater variation when it bloomed. Likewise, this phenological state presents a high correlation with the crop yield.

4.2.2. Comparison Between Trials

According to the preliminary sampling (development 1), the NDVI values varied from 0.78–0.81 for the field trial, while for the greenhouse they were about 0.73–0.79. This is because factors such as the leaf thickness, leaf age and leaf area index can influence the spectral response of the leaf [116]. Regarding the treatments T4 and T5 (nanofertilizers), they yielded an increase in the value of the index after the first application for both tests, since the application of ZnO nanofertilizers increases the chlorophyll content [111]. On the other hand, treatment 3 (chelates) in the field trial presented the lowest value of NDVIS in all phenological states, because it contained a concentration higher than the recommended concentration, causing a possible phytotoxicity in the plant [117].

In the flowering state, the different treatments determined a significant decrease in the index value in the two trials, as a product of the sensitivity to diseases that this state presents [118]. This agrees with studies on lupin and corn, in which the NDVI value decreased and varied significantly in this phenological state [99,115].

In the reproductive state, T5 in the field tests and T4 in the greenhouse tests indicated an increase in the value of NDVIS, surpassing the control treatment since nanofertilizers are useful for disease management. Finally, in the sheathed state, a decrease in the value of NDVIS was identified, which is usually observed when the crop is close to physiological maturity [119]. On the other hand, in a different study, a decay in the relation of rice grain yield with the values of the crop sensor was encountered, possibleydue to effects related to the decrease in the canopy in front of the sensor's field of view [120].

The criterion for discerning that the greenhouse environment had a better effect on the crop was based on the fact that the equipment was able to significantly differentiate between treatments, whereas in the field it was not. If we analyze the absolute values of the NDVI index (Figure 8), T4 and T5 always end up, in both cases, above the rest of the treatments in the final phenological stage, but this differentiation is greater in the greenhouse, meaning there is a greater separation in the results between treatments. Additionally, for T4, it can be observed that there is a greater drop between the vegetative development 2 stage and the flowering stage, but the plant is able to recover for the reproductive stage. On the other hand, we see that control follows a more regular evolution, always ending in the final phenological stage with lower vigor.

5. Conclusions

The use of geospatial tools in the cultivation of lupin allows for the spectral characterization of the effect of the application of nanofertilizers and Fe and Zn chelates. The use of these instruments made it possible to generate indices that allowedus to identify significant differences between treatments, as well as between phenological states.

From the field trial, four RGN orthomosaics were obtained, one for each phenological state. These were used to generate NDVI maps and obtain a total of 600 weighted NDVI values.

We can conclude that the vegetation indices (NDVI, TNDVI, GNDVI, GCI, DVI and RDVI) were efficient in spectrally characterizing the lupin crop under the application of nanofertilizers and Fe and Zn chelates in controlled trials. In each of the analyses, treatments T4 (nanofertilizers Fe and Zn 540 ppm) and T5 (nanofertilizers Fe and Zn 270 ppm), allowed us to obtain higher values with respect to the control. In the case of the vegetation indices NDVI and TNDVI, the treatments with nanofertilizers (T4 and T5) presented higher values, meaning that they improved the health status of the crop. Likewise, the GNDVI and GCI indices indicated higher values in the treatments with nanofertilizers. Therefore, it can be concluded that chlorophyll levels were higher, because these indices are sensitive to this parameter. Similarly, the vegetation indices DVI and RDVI presented higher values in treat-

ments T4 and T5, compared to the control (T1). That is, the application of nanofertilizers improved the cell structure of the culture.

Through the use of the spectroradiometer, it was possible to generate vegetation indices that allowed us to significantly differentiate between treatments applied to the cultivation of lupin in the field. The DVI and RDVI indices that use the NIR band established that the nanofertilizers (T5) did not alter the cell structure of the plant, while the GCI index that uses the green band identified a higher concentration of chlorophyll in the T4 treatment (therefore, increased pigmentation in the leaves). In terms of precision, the DVI and RDVI indices stood out compared to the GCI index since they differentiated three of the five treatments applied. On the other hand, the NDVI index obtained from the crop sensor indicated better pigmentation in the T4 treatment leaves, while the NDVIUAV presented a precision similar to the GCI index.

All of the indices obtained from the spectral signatures in the greenhouse and field tests efficiently distinguished between the different phenological states of the lupin crop. The NDVIE, TNDVI, RDVI and DVI indices only managed to significantly differentiate three of the four states analyzed, while the GNDVI and GCI indices presented greater sensitivity when distinguishing each phenological state. This established a decrease in pigmentation during the sheathed state, due to the proximity of senescence of the plant.

The indices calculated using spectral data efficiently distinguished between phenological states. In the greenhouse test, the DVI and RDVI indices presented greater precision to significantly differentiate the four phenological states, while in the field test the GNDVI and GCI indices indicated greater precision because they are more sensitive to chlorophyll content. Similarly, the NDVI index obtained using the multispectral camera (RGN, NDVI) significantly differentiated each state, which establishes the importance of spectral resolution when conducting studies on different crops.

Through the use of the spectroradiometer spectrum, it was possible to demonstrate that the application of Fe and Zn nanofertilizers implied an improvement in the structure and chlorophyll content of the leaf, and therefore in the development of the lupin plant in the greenhouse test. Contrarily, in the field trial the applied treatments did not yield an improvement in relation to treatment 1 (control). This may be related to environmental factors, such as temperature, light, relative humidity and application time, which influence the success of foliar fertilization. Additional treatment of T3 caused a deterioration in chlorophyll, as well as in the cellular structure of the plant in both tests. On the other hand, according to the indices obtained from spectral data (NDVIS and NDVIUAV), a decrease in vigor and health of the plant was established in the flowering state due to the susceptibility to diseases that this state presents.

Measurements conducted in the greenhouse evidenced that the application of nanofertilizers at a concentration of 540 ppm exhibited significant effectiveness; however, this concentration was less effective in field conditions. Future work should focus on improving the retention mechanisms of nanofertilizers under less controlled environmental conditions, such as the influence of wind or precipitation.

Future work may propose the use of hyperspectral cameras in order to expand the range of spectral bands available from the drone and, furthermore, to extend the study to larger surface areas. Similarly, this methodology may be applied to other types of crops to non-invasively analyze the effects of new treatments on different agricultural systems.

Author Contributions: Conceptualization I.S.-G., E.M.-H. and C.E.F.; Methodology I.S.-G. and C.E.F.; Software I.S.-G.; Formal Analysis I.S.-G., E.M.-H. and C.E.F.; Investigation I.S.-G., E.M.-H. and C.E.F.; Data Curation I.S.-G.; writing—original draft preparation I.S.-G.; writing—review and editing I.S.-G., E.M.-H., C.E.F., M.G.-D. and T.T.; Editing Supervision I.S.-G., E.M.-H., C.E.F., M.G.-D. and T.T. All authors have read and agreed to the published version of the manuscript.

Funding: This research received no external funding.

Data Availability Statement: https://drive.google.com/drive/folders/1BUV3-knOJ4Tj-IXFQYoMdqBAq0KhGPFN?usp=sharing accessed on 12 February 2025.

Acknowledgments: The authors would like to express their gratitude to Kevin Martinez and Karina Yanchatipán for their support in the development of the study.

Conflicts of Interest: The authors declare no conflicts of interest.

References

1. Chartuni, E.; de Assis de Carvalho, F.; Marcal, D.; Ruz, E. Precision agriculture: New tools to improve technology management in agricultural enterprises. *Comuniica Mag.* **2007**, *2007*, 24–31.
2. Hedley, C. The role of precision agriculture for improved nutrient management on farms. *J. Sci. Food Agric.* **2015**, *95*, 12–19. [CrossRef] [PubMed]
3. Köksal, Ö.; Tekinerdogan, B. Architecture design approach for IoT-based farm management information systems. *Precis. Agric.* **2019**, *20*, 926–958. [CrossRef]
4. Bhakta, I.; Phadikar, S.; Majumder, K. State-of-the-art technologies in precision agriculture: A systematic review. *J. Sci. Food Agric.* **2019**, *99*, 4878–4888. [CrossRef]
5. Croner, C.M.; Sperling, J.; Broome, F.R. Geographic information systems (GIS): New perspectives in understanding human health and environmental relationships. *Stat. Med.* **1996**, *15*, 1961–1977. [CrossRef]
6. Xue, Y.; Cracknell, A.P.; Guo, H.D. Telegeoprocessing: The integration of remote sensing, geographic information system (GIS), global positioning system (GPS) and telecommunication. *Int. J. Remote Sens.* **2002**, *23*, 1851–1893. [CrossRef]
7. Seelan, S.K.; Laguette, S.; Casady, G.M.; Seielstad, G.A. Remote sensing applications for precision agriculture: A learning community approach. *Remote Sens. Environ.* **2003**, *88*, 157–169. [CrossRef]
8. Sonti, S.H. Application of geographic information system (GIS) in forest management. *J. Geogr. Nat. Disasters* **2015**, *5*, 1000145.
9. Banu, S. Precision agriculture: Tomorrow's technology for today's farmer. *J. Food Process. Technol.* **2015**, *6*, 8.
10. Thakur, J.K.; Singh, S.K.; Ekanthalu, V.S. Integrating remote sensing, geographic information systems and global positioning system techniques with hydrological modeling. *Appl. Water Sci.* **2017**, *7*, 1595–1608. [CrossRef]
11. Roberson, G.T. Precision agriculture technology for horticultural crop production. *HortTechnology* **2000**, *10*, 448–451. [CrossRef]
12. Fulton, J.P.; Port, K.; Shannon, D.K.; Clay, D.E.; Kitchen, N.R. Precision agriculture data management. In *Precision Agriculture Basics*; John Wiley & Sons: Hoboken, NJ, USA, 2018; pp. 169–188.
13. Lund, E.D.; Christy, C.D.; Drummond, P.E. Practical applications of soil electrical conductivity mapping. *Precis. Agric.* **1999**, *99*, 771–779.
14. Abdullahi, H.S.; Mahieddine, F.; Sheriff, R.E. Technology impact on agricultural productivity: A review of precision agriculture using unmanned aerial vehicles. In *Wireless and Satellite Systems, Proceedings of the 7th International Conference, WiSATS 2015, Bradford, UK, 6–7 July 2015*; Springer: Cham, Switzerland, 2015; pp. 388–400.
15. Weiss, J.; Takhistov, P.; McClements, D.J. Functional materials in food nanotechnology. *J. Food Sci.* **2006**, *71*, R107–R116. [CrossRef]
16. Pal, S.L.; Jana, U.; Manna, P.K.; Mohanta, G.P.; Manavalan, R. Nanoparticle: An overview of preparation and characterization. *J. Appl. Pharm. Sci.* **2011**, *1*, 228–234.
17. Sawhney, A.P.S.; Condon, B.; Singh, K.V.; Pang, S.S.; Li, G.; Hui, D. Modern applications of nanotechnology in textiles. *Text. Res. J.* **2008**, *78*, 731–739. [CrossRef]
18. Khan, Y.; Sadia, H.; Ali Shah, S.Z.; Khan, M.N.; Shah, A.A.; Ullah, N.; Ullah, M.F.; Bibi, H.; Bafakeeh, O.T.; Ben Khedher, N.; et al. Classification, synthetic, and characterization approaches to nanoparticles, and their applications in various fields of nanotechnology: A review. *Catalysts* **2022**, *12*, 1386. [CrossRef]
19. Mekuye, B.; Abera, B. Nanomaterials: An overview of synthesis, classification, characterization, and applications. *Nano Sel.* **2023**, *4*, 486–501. [CrossRef]
20. Ahire, S.A.; Bachhav, A.A.; Pawar, T.B.; Jagdale, B.S.; Patil, A.V.; Koli, P.B. The Augmentation of nanotechnology era: A concise review on fundamental concepts of nanotechnology and applications in material science and technology. *Results Chem.* **2022**, *4*, 100633. [CrossRef]
21. Debut, A.; Toulkeridis, T.; Vaca, A.V.; Arroyo, C.R. Origin of color variations of thin, nano-sized layers of volcanic cinder from the Sierra Negra Volcano of the Galapagos Islands. *Uniciencia* **2021**, *35*, 210–222. [CrossRef]
22. Herrera, E.M.; Lucio, S.; Izquierdo, A.; Arroyo, G.; Stael, C.; Toulkeridis, T. Application of Multicomponent Nanoparticles Synthesized with Andean Blackberry Fruit Extract (*Rubus Glaucus*) NPs (Ca, Fe, Mg-Rg) for Oyster Mushrooms (*Pleurotus Ostreatus*). In Proceedings of the XVIII Multidisciplinary International Congress on Science and Technology, Leiden, The Netherlands, 27–29 September 2023; Springer Nature: Cham, Switzerland, 2023; pp. 149–162.

23. Raliya, R.; Saharan, V.; Dimkpa, C.; Biswas, P. Nanofertilizer for precision and sustainable agriculture: Current state and future perspectives. *J. Agric. Food Chem.* **2017**, *66*, 6487–6503. [CrossRef]
24. Arguello, M. Growth promotion of Capsicum annuum plants by zinc oxide nanoparticles. *Nova Sci.* **2016**, *8*, 140–156.
25. Zulfiqar, F.; Navarro, M.; Ashraf, M.; Akram, N.A.; Munné-Bosch, S. Nanofertilizer use for sustainable agriculture: Advantages and limitations. *Plant Sci.* **2019**, *289*, 110270. [CrossRef]
26. Liu, R.; Lal, R. Potentials of engineered nanoparticles as fertilizers for increasing agronomic productions. *Sci. Total Environ.* **2015**, *514*, 131–139. [CrossRef]
27. Fatima, F.; Hashim, A.; Anees, S. Efficacy of nanoparticles as nanofertilizer production: A review. *Environ. Sci. Pollut. Res.* **2021**, *28*, 1292–1303. [CrossRef] [PubMed]
28. Mahapatra, D.M.; Satapathy, K.C.; Panda, B. Biofertilizers and nanofertilizers for sustainable agriculture: Phycoprospects and challenges. *Sci. Total Environ.* **2022**, *803*, 149990. [CrossRef]
29. Kumar, Y.; Tiwari, K.N.; Singh, T.; Raliya, R. Nanofertilizers and their role in sustainable agriculture. *Ann. Plant Soil Res.* **2021**, *23*, 238–255. [CrossRef]
30. Babu, S.; Singh, R.; Yadav, D.; Rathore, S.S.; Raj, R.; Avasthe, R.; Yadav, S.K.; Das, A.; Yadav, V.; Yadav, B.; et al. Nanofertilizers for agricultural and environmental sustainability. *Chemosphere* **2022**, *292*, 133451. [CrossRef] [PubMed]
31. Nongbet, A.; Mishra, A.K.; Mohanta, Y.K.; Mahanta, S.; Ray, M.K.; Khan, M.; Baek, K.-H.; Chakrabartty, I. Nanofertilizers: A smart and sustainable attribute to modern agriculture. *Plants* **2022**, *11*, 2587. [CrossRef] [PubMed]
32. Manjunatha, S.B.; Biradar, D.P.; Aladakatti, Y.R. Nanotechnology and its applications in agriculture: A review. *J. Farm Sci.* **2016**, *29*, 1–13.
33. Dimkpa, C.; Bindraban, P.S. Nanofertilizers: New Products for the Industry. *J. Agric. Food Chem.* **2017**, *66*, 6462–6473. [CrossRef]
34. Guha, T.; Gopal, G.; Kundu, R.; Mukherjee, A. Nanocomposites for delivering agrochemicals: A comprehensive review. *J. Agric. Food Chem.* **2020**, *68*, 3691–3702. [CrossRef] [PubMed]
35. Semenova, N.A.; Burmistrov, D.E.; Shumeyko, S.A.; Gudkov, S.V. Fertilizers based on nanoparticles as sources of macro-and microelements for plant crop growth: A review. *Agronomy* **2024**, *14*, 1646. [CrossRef]
36. Pudhuvai, B.; Koul, B.; Das, R.; Shah, M.P. Nano-Fertilizers (NFs) for resurgence in nutrient use efficiency (NUE): A sustainable agricultural strategy. *Curr. Pollut. Rep.* **2024**, *11*, 1. [CrossRef]
37. Ndaba, B.; Akindolire, M.; Botha, T.L.; Roopnarain, A. The Use of Nanofertilizers as Micronutrients to Improve Marginal Soils and Crop Production. In *The Marginal Soils of Africa: Rethinking Uses, Management and Reclamation*; Springer Nature: Cham, Switzerland, 2024; pp. 205–227.
38. Sinfield, J.V.; Fagerman, D.; Colic, O. Evaluation of sensing technologies for on-the-go detection of macro-nutrients in cultivated soils. *Comput. Electron. Agric.* **2010**, *70*, 1–18. [CrossRef]
39. Ejaz, M.; Waqas, R.; Butt, M.; Rehman, S.U.; Manan, A. Role of macro-nutrients and micro-nutrients in enhancing the quality of tomato. *Int. J. Agron. Vet. Med. Sci.* **2011**, *5*, 401–404. [CrossRef]
40. Singh, R.P.; Mishra, S.K. Available macro nutrients (N, P, K and S) in the soils of Chiraigaon block of district Varanasi (UP) in relation to soil characteristics. *Indian J. Sci. Res.* **2012**, *3*, 97–100.
41. Toor, M.D.; Adnan, M.; Rehman, F.U.; Tahir, R.; Saeed, M.S.; Khan, A.U.; Pareek, V. Nutrients and their importance in agriculture crop production: A review. *Ind. J. Pure App. Biosci.* **2021**, *9*, 1–6. [CrossRef]
42. Rout, G.R.; Sahoo, S. Role of iron in plant growth and metabolism. *Rev. Agric. Sci.* **2015**, *3*, 1–24. [CrossRef]
43. Imsande, J. Iron, sulfur, and chlorophyll deficiencies: A need for an integrative approach in plant physiology. *Physiol. Plant.* **1998**, *103*, 139–144. [CrossRef]
44. Das, S.K. Role of micronutrient in rice cultivation and management strategy in organic agriculture—A reappraisal. *Agric. Sci.* **2014**, *5*, 48363. [CrossRef]
45. Magri, E.; Gugelmin, E.K.; Grabarski, F.A.P.; Barbosa, J.Z.; Auler, A.C.; Wendling, I.; Prior, S.A.; Valduga, A.T.; Motta, A.C.V. Manganese hyperaccumulation capacity of Ilex paraguariensis A. St. Hil. and occurrence of interveinal chlorosis induced by transient toxicity. *Ecotoxicol. Environ. Saf.* **2020**, *203*, 111010. [CrossRef]
46. Zeiger, E.; Taiz, L. *Fisiología Vegetal*; En L. T. *Zeiger*; Book Print Digital, SA: Los Angeles, CA, USA, 2006.
47. Zhao, W.; Yang, P.; Kang, L.; Cui, F. Different pathogenicities of Rice stripe virus from the insect vector and from viruliferous plants. *New Phytol.* **2016**, *210*, 196–207. [CrossRef]
48. Rajendran, C.; Hepziba, S.J.; Ramamoorthy, K. *Nutritional and Physiological Disorders in Crop Plants*; Scientific Publishers: Jodhpur, India, 2009.
49. Ounis, S.; Turóczi, G.; Kiss, J. Arthropod Pests, Nematodes, and Microbial Pathogens of Okra (Abelmoschus esculentus) and Their Management—A Review. *Agronomy* **2024**, *14*, 2841. [CrossRef]
50. Vasile, D.; Enescu, R.; Apafaian, A.; Coman, S.; Scarlatescu, V.; Crisan, V. Bioaccumulation of long-term atmospheric heavy metal pollution within the Carpathian arch: Monumental trees and their leaves memoir. *iFor.-Biogeosci. For.* **2024**, *17*, 370. [CrossRef]

51. Mora Villacís, M.G.; Cañarte Ruiz, D.A.; Kirby, E.; Maiguashca Guzmán, J.A.; Toulkeridis, T. Index Relationship of Vegetation with the Development of a Quinoa Crop (Chenopodium quinoa) in its First Phenological Stages in Central Ecuador Based on GIS Techniques. In Proceedings of the 2020 7th International Conference on eDemocracy and eGovernment, ICEDEG 2020, Buenos Aires, Argentina, 22–24 April 2020; pp. 190–199.
52. Muñoz, E.B.; Luna-Vital, D.A.; Fornasini, M.; Baldeón, M.E.; de Mejia, E.G. Gamma-conglutin peptides from Andean lupin legume (*Lupinus mutabilis* Sweet) enhanced glucose uptake and reduced gluconeogenesis in vitro. *J. Funct. Foods* **2018**, *45*, 339–347. [CrossRef]
53. Murgueitio-Herrera, E.; Falconí, C.E.; Cumbal, L.; Gómez, J.; Yanchatipán, K.; Tapia, A.; Martínez, K.; Sinde-Gonzalez, I.; Toulkeridis, T. Synthesis of iron, zinc, and manganese nanofertilizers, using Andean blueberry extract, and their effect in the growth of cabbage and lupin plants. *Nanomaterials* **2022**, *12*, 1921. [CrossRef] [PubMed]
54. Miano, A.C.; García, J.A.; Augusto, P.E.D. Correlation between morphology, hydration kinetics and mathematical models on Andean lupin (*Lupinus mutabilis* Sweet) grains. *LWT-Food Sci. Technol.* **2015**, *61*, 290–298. [CrossRef]
55. Mikić, A.; Ćupina, B.; Mihailović, V.; Krstić, Đ.; Antanasović, S.; Zorić, L.; Đorđević, V.; Perić, V.; Srebrić, M. Intercropping white (*Lupinus albus*) and Andean (*Lupinus mutabilis*) lupins with other annual cool season legumes for forage production. *S. Afr. J. Bot.* **2013**, *89*, 296–300. [CrossRef]
56. Jacobsen, S.E.; Mujica, A. Geographical distribution of the Andean lupin (*Lupinus mutabilis* Sweet). *Plant Genet. Resour. Newsl.* **2008**, *155*, 1–8.
57. Montagnini, F.; Grover, E.C.; Hering, P.; Bachmann, G. Conclusions: Agroforestry for Biodiversity Conservation and Food Sovereignty—Lessons Learned and Pending Challenges. In *Integrating Landscapes: Agroforestry for Biodiversity Conservation and Food Sovereignty*; Springer Nature: Cham, Switzerland, 2024; pp. 707–732.
58. Rey-Lema, D.M.; Peña-Galindo, A. Food Sovereignty: An Analysis of the Cañamomo Lomaprieta Indigenous Reservation, Local Resistances against Domination. *Inven. Iudicandi* **2024**, *19*, 10–24. [CrossRef]
59. Mudombi-Rusinamhodzi, G.; Rusinamhodzi, L. Food sovereignty in sub-Saharan Africa: Reality, relevance, and practicality. *Front. Agron.* **2022**, *4*, 957011. [CrossRef]
60. Swinbank, V.A.; Swinbank, V.A. Women feed the world: Biodiversity and culinary diversity/food security and food sovereignty. In *Women's Food Matters: Stirring the Pot*; Palgrave Macmillan: Cham, Switzerland, 2021; pp. 187–218.
61. Cusworth, G.; Garnett, T.; Lorimer, J. Legume dreams: The contested futures of sustainable plant-based food systems in Europe. *Glob. Environ. Change* **2021**, *69*, 102321. [CrossRef]
62. Villacrés, E.; Rubio, A.; Egas, L.; Segovia, G. *Usos Alternativos del Chocho*; INIAP: Quito, Ecuador, 2006.
63. Giunta, I. Food sovereignty in Ecuador: Peasant struggles and the challenge of institutionalization. *J. Peasant Stud.* **2014**, *41*, 1201–1224. [CrossRef]
64. Peña, K. Social movements, the state, and the making of food sovereignty in Ecuador. *Lat. Am. Perspect.* **2016**, *43*, 221–237. [CrossRef]
65. Falconí, C.E.; Visser, R.G.; van Heusden, A.W. Phenotypic, molecular, and pathological characterization of Colletotrichum acutatum associated with Andean lupin and tamarillo in the Ecuadorian Andes. *Plant Dis.* **2013**, *97*, 819–827. [CrossRef]
66. Carlos, M.M.; Liliana, P.; Cerda-Mejía, A.; Daniele, R. The Agrifood network of lupin bean (*Lupinus mutabilis*) in Ecuador: A characterization of the value chain with a socioeconomic and productive perspective. In Proceedings of the 2018 Seventh AIEAA Conference, Conegliano, Italy, 14–15 June 2018.
67. Struelens, Q.; Mina, D.; Dangles, O. Combined effects of landscape composition and pesticide use on herbivore and pollinator functions in smallholder farms. *CABI Agric. Biosci.* **2021**, *2*, 7. [CrossRef]
68. Blackmore, I.; Rivera, C.; Waters, W.F.; Iannotti, L.; Lesorogol, C. The impact of seasonality and climate variability on livelihood security in the Ecuadorian Andes. *Clim. Risk Manag.* **2021**, *32*, 100279. [CrossRef]
69. Caicedo, C.; Peralta, E. *Zonificación Potencial, Sistemas de Producción y Procesamiento Artesanal del Choho (Lupinus mutabilis Sweet) en Ecuador*; INIAP: Quito, Ecuador, 2000.
70. Falconí, C. *Lupinus mutabilis* in Ecuador with Special Emphasis on Anthracnose Resistance. Ph.D. Thesis, Wageningen University, Wageningen, The Netherlands, 2012.
71. Horning, N. *Introduction Remotely Sensed Data Sets for Ecological Modeling Accuracy Assessment and Validation*; New York, NY, USA, 2008; pp. 2986–2993.
72. Schwertfirm, G.; Schneider, M.; Haase, F.; Riedel, C.; Lazzaro, M.; Ruge-Wehling, B.; Schweizer, G. Genome-wide association study revealed significant SNPs for anthracnose resistance, seed alkaloids and protein content in white lupin. *Theor. Appl. Genet.* **2024**, *137*, 155. [CrossRef] [PubMed]
73. dos Santos, A.A.; de Freitas, M.B.; Ribeiro, C.F.; Poltronieri, A.S.; Stadnik, M.J. Silver Nanoparticles Reduce Anthracnose Severity and Promote Growth of Bean Plants (*Phaseolus vulgaris*). *Agronomy* **2024**, *14*, 2806. [CrossRef]
74. Kosev, V.; Vasileva, V.; Popović, V. New variety of white lupin Monica (*Lupinus albus* L.). *Genetika* **2024**, *56*, 347–356. [CrossRef]
75. Brisco, B.; Brown, R.J.; Hirose, T.; McNairn, H.; Staenz, K. Precision agriculture and the role of remote sensing: A review. *Can. J. Remote Sens.* **1998**, *24*, 315–327. [CrossRef]

76. Segarra, J.; Buchaillot, M.L.; Araus, J.L.; Kefauver, S.C. Remote sensing for precision agriculture: Sentinel-2 improved features and applications. *Agronomy* **2020**, *10*, 641. [CrossRef]
77. Khanal, S.; Fulton, J.; Shearer, S. An overview of current and potential applications of thermal remote sensing in precision agriculture. *Comput. Electron. Agric.* **2017**, *139*, 22–32. [CrossRef]
78. Torres, B.; Andrade, V.; Heredia-R, M.; Toulkeridis, T.; Estupiñán, K.; Luna, M.; Bravo, C.; García, A. Productive Livestock Characterization and Recommendations for Good Practices Focused on the Achievement of the SDGs in the Ecuadorian Amazon. *Sustainability* **2022**, *14*, 10738. [CrossRef]
79. Saiz-Rubio, V.; Rovira-Más, F. From smart farming towards agriculture 5.0: A review on crop data management. *Agronomy* **2020**, *10*, 207. [CrossRef]
80. Nebiker, S.; Annen, A.; Scherrer, M.; Oesch, D. A light-weight multispectral sensor for micro UAV—Opportunities for very high resolution airborne remote sensing. *Int. Arch. Photogramm. Remote Sens. Spat. Inf. Sci.* **2008**, *37*, 1193–1200.
81. Feng, Q.; Liu, J.; Gong, J. UAV remote sensing for urban vegetation mapping using random forest and texture analysis. *Remote Sens.* **2015**, *7*, 1074–1094. [CrossRef]
82. Hunt, R.; Daughtry, C. What good are unmanned aircraft systems for agricultural remote sensing and precision agriculture? *Int. J. Remote Sens.* **2017**, *39*, 5345–5376. [CrossRef]
83. Harle, S.; Bhagat, A.; Dash, A.K. Remote Sensing Revolution: Mapping Land Productivity and Vegetation Trends with Unmanned Aerial Vehicles (UAVs). *Curr. Appl. Mater.* **2024**, *3*, e070224226752. [CrossRef]
84. Fuentes-Peñailillo, F.; Gutter, K.; Vega, R.; Silva, G.C. Transformative technologies in digital agriculture: Leveraging Internet of Things, remote sensing, and artificial intelligence for smart crop management. *J. Sens. Actuator Netw.* **2024**, *13*, 39. [CrossRef]
85. Selmy, S.A.; Kucher, D.E.; Yang, Y. Geospatial Data: Acquisition, Applications, and Challenges. In *Remote Sensing-Methods and Applications: Methods and Applications*; Intechopen: London, UK, 2025; p. 61.
86. Almohsen, A.S. Challenges facing the use of remote sensing technologies in the construction industry: A review. *Buildings* **2024**, *14*, 2861. [CrossRef]
87. Gholizadeh, A.; Kopačková, V. Detecting vegetation stress as a soil contamination proxy: A review of optical proximal and remote sensing techniques. *Int. J. Environ. Sci. Technol.* **2019**, *16*, 2511–2524. [CrossRef]
88. Pu, R. *Hyperspectral Remote Sensing: Fundamentals and Practices*; Taylor & Francis Group: Indianapolis, IN, USA, 2017.
89. Weiss, M.; Jacob, F. Remote sensing for agricultural applications: A meta-review. *Remote Sens. Environ.* **2020**, *236*, 111402. [CrossRef]
90. Viera-Torres, M.; Sinde-González, I.; Gil-Docampo, M.; Bravo, V.; Toulkeridis, T. Generation of the base line in the early detection of bud rot and the red ring disease in oil palms by geospatial technologies. *Remote Sens.* **2020**, *12*, 3229. [CrossRef]
91. Yang, C. Remote Sensing and Precision Agriculture Technologies for Crop Disease Detection and Management with a Practical Application Example. *Engineering* **2020**, *6*, 528–532. [CrossRef]
92. Peng, M.; Liu, Y.; Khan, A.; Ahmed, B.; Sarker, S.K.; Ghadi, Y.Y.; Bhatti, U.A.; Al-Razgan, M.; Ali, Y.A. Crop monitoring using remote sensing land use and land change data: Comparative analysis of deep learning methods using pre-trained CNN models. *Big Data Res.* **2024**, *36*, 100448. [CrossRef]
93. Han, H.; Liu, Z.; Li, J.; Zeng, Z. Challenges in remote sensing based climate and crop monitoring: Navigating the complexities using AI. *J. Cloud Comput.* **2024**, *13*, 34. [CrossRef]
94. Ding, W.; Abdel-Basset, M.; Alrashdi, I.; Hawash, H. Next generation of computer vision for plant disease monitoring in precision agriculture: A contemporary survey, taxonomy, experiments, and future direction. *Inf. Sci.* **2024**, *665*, 120338. [CrossRef]
95. Psomas, A.; Zimmermann, N.E.; Kneubühler, M.; Kellenberger, T.; Itten, K. Seasonal variability in spectral reflectance for discriminating grasslands along a dry-mesic gradient in Switzerland. In Proceedings of the 4th EARSEL Workshop on Imaging Spectroscopy, Warsaw, Poland, 27–30 April 2005; pp. 709–722.
96. Manevski, K.; Manakos, I.; Petropoulos, G.P.; Kalaitzidis, C. Discrimination of common Mediterranean plant species using field spectroradiometry. *Int. J. Appl. Earth Obs. Geoinf.* **2011**, *13*, 922–933. [CrossRef]
97. Tapia-Silva, F.O.; Itzerott, S.; Foerster, S.; Kuhlmann, B.; Kreibich, H. Estimation of flood losses to agricultural crops using remote sensing. *Phys. Chem. Earth Parts A/B/C* **2011**, *36*, 253–265. [CrossRef]
98. Kosewska, A.; Nietupski, M.; Nijak, K.; Skalski, T. Effect of plant protection on assemblages of ground beetles (Coleoptera, Carabidae) in pea (*Pisum* L.) and lupin (*Lupinus* L.) crops. *Period. Biol.* **2016**, *118*, 213–222. [CrossRef]
99. Sinde-González, I.; Falconí-Saá, C.E.; Luna-Granizo, P.; Godoy-Guanín, L.; Gil-Docampo, M.D.L.L.; Maiguashca, J.; Nato, R. Spectral analysis of the phenological stages of *Lupinus mutabilis* through spectroradiometry and unmanned aerial vehicle imaging with different physical disinfection pretreatments of seeds. *Geocarto Int.* **2021**, *37*, 7143–7160. [CrossRef]
100. Toulkeridis, T.; Chunga, K.; Rentería, W.; Rodriguez, F.; Mato, F.; Nikolaou, S.; Cruz D'Howitt, M.; Besenzon, D.; Ruiz, H.; Parra, H.; et al. The 7.8 Mw Earthquake and Tsunami of the 16th April 2016 in Ecuador—Seismic evaluation, geological field survey and economic implications. *Sci. Tsunami Hazards* **2017**, *36*, 197–242.
101. Toulkeridis, T.; Zach, I. Wind directions of volcanic ash-charged clouds in Ecuador—Implications for the public and flight safety. *Geomat. Nat. Hazards Risks* **2017**, *8*, 242–256. [CrossRef]

102. Macías, L.; Quiñonez-Macías, M.; Toulkeridis, T.; Pastor, J.L. Characterization and geophysical evaluation of the recent 2023 Alausí Landslide in the Northern Andes of Ecuador. *Landslides* **2024**, *21*, 529–540. [CrossRef]
103. Mapir Camera Control (MCC). Mapir. Process Tab. Available online: https://mapir.gitbook.io/mapir-camera-control-mcc/interface-tabs/process-tab (accessed on 7 February 2025).
104. Tucker, C.J. Red and photographic infrared linear combinations for monitoring vegetation. *Remote Sens. Environ.* **1979**, *8*, 127–150. [CrossRef]
105. Pettorelli, N. *The Normalized Difference Vegetation Index*; Oxford University Press: Oxford, UK, 2013.
106. Naji, T.A. Study of vegetation cover distribution using DVI, PVI, WDVI indices with 2D-space plot. In *Journal of Physics: Conference Series*; IOP Publishing: Bristol, UK, 2018; Volume 1003, p. 012083.
107. Melillos, G.; Themistocleous, K.; Hadjimitsis, D.G. Detecting underground structures in vegetation indices: MSR, RDVI, OSAVI, IRG, time series using histograms. In Proceedings of the Eighth International Conference on Remote Sensing and Geoinformation of the Environment (RSCy2020), Paphos, Cyprus, 16–18 March 2020; International Society for Optics and Photonics: Bellingham, WA, UA, 2020; Volume 11524, p. 115241P.
108. Agapiou, A.; Hadjimitsis, D.; Alexakis, D. Evaluation of Broadband and Narrowband Vegetation Indices for the Identification of Archaeological Crop Marks. *Remote Sens.* **2012**, *4*, 3892–3919. [CrossRef]
109. Simbaña, E.; Tello, J. Estimación de Biomasa y Análisis de la Variación Espectral de Chocho (*Lupinus mutabilis* Sweet) por la Aplicación de Métodos de Control Biológico en dos Ensayos Controlados Utilizando Sensores Remotos. Bachelor's Thesis, Universidad de las Fuerzas Armadas-ESPE, Sangolquí, Ecuador, 2020.
110. Abd El-Azeim, M.M.; Sherif, M.A.; Hussien, M.S.; Tantawy, I.A.A.; Bashandy, S.O. Impacts of nano-and non-nanofertilizers on potato quality and productivity. *Acta Ecol. Sin.* **2020**, *40*, 388–397. [CrossRef]
111. Tarafdar, J.; Raliya, R. Development of Zinc Nanofertilizer to Enhance Crop Production in Pearl Millet (*Pennisetum americanum*). *Agric. Res.* **2014**, *3*, 257–262. [CrossRef]
112. Klaas, P. Applying conventional vegetation vigor indices to uas-derived orthomosaics: Issues and considerations. In Proceedings of the 12th International Conference for Precision Agriculture, Sacramento, CA, USA, 20–23 July 2014; Volume 13.
113. Haboudane, D.; Miller, J. Hyperspectral vegetation indices and novel algorithms for predicting green LAI of crop canopies: Modeling and validation in the context of precision agriculture. *Remote Sens. Environ.* **2004**, *90*, 337–352. [CrossRef]
114. Matamoros, F.; Falconí, C. *Aplicación de Calor Seco en Semillas de Chocho Lupinus mutabilis var. Iniap-540 Andino y su Efecto en la Reduccion de Antracnosis en Invernadero*; Universidad de las Fuerzas Armadas ESPE: Sangolquí, Ecuador, 2018; p. 10.
115. De la Casa, A.; Ovando, G. Normalized Difference Vegetation Index (NDVI) and Phenological Data Integration to Estimate County Yield of Corn in Córdoba, Argentina. *Agric. Tec.* **2007**, *67*, 362–371.
116. Katsoulas, N.; Elvanidi, A. Crop reflectance monitoring as a tool for water stress detection in greenhouses: A review. *Biosyst. Eng.* **2016**, *151*, 374–398. [CrossRef]
117. Molina, E.; Meléndez, G. *Fertilización Foliar: Principios y Aplicaciones*; Centro de Investigaciones Agronomicas: Los Angeles, CA, USA, 2002; pp. 36–37.
118. Falconí, C.; Bracho, K. *Efecto del Pretratamiento de Semillas con Calor Seco, Para el Control de Antracnosis y en el Rendimiento de Chocho*; ESPE: Sangolquí, Ecuador, 2019; p. 27.
119. Guamán, A. Monitoreo de Maíz duro Mediante Índices de Vegetación Obtenidos por Imágenes. Bachelor's Thesis, Universidad Central del Ecuador, Quito, Ecuador, 2018; p. 65.
120. Ali, M.; Thind, H. Prediction of dry direct-seeded rice yields using chlorophyll meter, leaf color chart and GreenSeeker optical sensor in northwestern India. *Field Crops Res.* **2014**, *5*, 11–15. [CrossRef]